International Core Journal of Engineering Volume 7 Issue 5, 2021
ISSN: 2414-1895 DOI: 10.6919/ICJE.202105_7(5).0012

A Fuzzy Adaptive Filter with the Student's t Distribution-based Trajectory Tracking for Inspection Wall-climbing Robot

Xin Lai, Guorui Zhu*

Southwest Petroleum University, Chengdu, Sichuan, 610500, China.

*zhgr1995@163.com

Abstract

To address the problem of measurement noise interference in the trajectory tracking process of a wall-climbing robot (WCR), a fuzzy adaptive robust Student's t-based extended Kalman filter (AFSTEKF) is proposed. The measurement noise of the extended Kalman filter (EKF) is modeled with a Student' s t distribution instead of a Gaussian distribution. Three kinds of filters are considered for comparison. Simulation results show that proposed algorithm is more robust with accuracy than existing state-of-the-art filters.

Keywords

Kalman Filter; Student's T Distribution; Wall-climbing Robot (WCR).

1. Introduction

Nonlinear filtering has been attracting considerable research interest because it plays an important role in many applications with inherent non-linearities such as target tracking, control and signal processing. For a general nonlinear system, a closed form solution of the posterior filtering probability density function (PDF) is often not available, so that the optimal solution doesn't exist and approximate approaches are necessary to design a suboptimal nonlinear filter. Gaussian approximation (GA) to the posterior filtering PDF is the most common approach because its corresponding Gaussian approximate filter provides tradeoffs between computational complexity and estimation accuracy in many practical applications. Several forms of GA filters have been studied, including the extended Kalman filter (EKF) [1], unscented Kalman filter (UKF) [2], cubature Kalman filter (CKF) [3] and their variants. These nonlinear filters usually only consider nonlinear systems with Gaussian distribution for the process noise and measurement noise, but their performance may be degraded by external environmental interference in some practical engineering applications with heavy tail process and measurement noise. For example, measurement information is typically used when tracking agile targets, including outliers from unreliable sensors.

The trajectory tracking of an inspection WCR often uses the Kalman filter to obtain the optimal solution in the sense of minimum variance of a linear system. The EKF linearizes the nonlinear system through the first-order Taylor expansion, then a Kalman filter is used for the linearized system. The performance and estimation quality of the EKF depend on the correct prior knowledge of the process and measurement noise covariance matrices. Because of its low computational complexity, the EKF has been widely used in theoretical research and practical engineering applications. However, not all practical applications can use the EKF, considering that the nonlinear state transfer equation and observation equation and their corresponding functions are differentiable or continuous, the EKF can not provide more accurate approximations, resulting in large calculation errors, so the EKF is more suitable for practical engineering applications with lower accuracy.

ISSN: 2414-1895 DOI: 10.6919/ICJE.202105_7(5).0012

There is an abnormal value of noise when a WCR is applied in the field environment. To solve this problem, such noise including outliers can be modelled by a heavy-tailed Student's t distribution. Some Student's t filters have been studied in the signal processing community. A high-accuracy gyroscope and accelerometer based inertial navigation system (INS) is the most common method for WCR navigation. However, the navigation error of an WCR is accumulated over time due to the drifts of the employed inertial sensors [4], which may lead to unbounded increase in the localization error (LE). Li et al. [5] proposed a robust leader–slave cooperative navigation (CN) algorithm based on the Student's t extended Kalman filter (STEKF) and applied it to an autonomous underwater vehicle (AUV). The effectiveness of the proposed CN algorithm is evaluated on the field test data, and the performance with different DOF values, which determines the tail behavior of the Students't distribution is compared and analyzed.

The remainder of this paper is organized as follows. In Section 2, the kinematics equation of the WCR is introduced; In Section 3, we present the simulation test results that demonstrate the validity of the robust algorithm for trajectory tracking of the WCR based on the Student's t distribution. We also propose a lateral comparison method, which can effectively compare the characteristics of different filtering algorithms. The lateral comparison method includes the comparison of three parameters: trajectories of the target, implementation times of the single step run and root-mean-square error; Section 4 concludes the paper with a summary of findings.

2. Methods

2.1 Kinematic model of WCR

The state equation of the WCR is as follows,

$$\begin{bmatrix}\dot{x}\\ \dot{y}\\ \dot{\theta}\end{bmatrix}=\begin{bmatrix}\cos\theta & 0\\ \sin\theta & 0\\ 0 & 1\end{bmatrix}\begin{bmatrix}v_c\\ \omega\end{bmatrix} \tag{1}$$

where $[\dot{x},\dot{y},\dot{\theta}]^T$ is the generalized coordinate velocity of the WCR, denotes as $\dot{q}$, and $(\ )^T$ denotes vector transpose; $[v_c,\omega]^T$ is the centroid velocity vector of the WCR, and $[v_c,\omega]^T$ denotes as V; the transformation matrix between the generalized coordinates velocity of the WCR and the centroid velocity of the robot's coordinates is denoted as S(q), so that we can obtain,

$$\dot{q}=S(q)V \tag{2}$$

$\boldsymbol{q}_r=[x_r,y_r,\theta_r]^T$ is the expected position vector of the trajectory tracking, and $\boldsymbol{q}_e$ is the expected position, then $\boldsymbol{q}_e$ is as follows,

$$\boldsymbol{q}_e=\boldsymbol{q}-\boldsymbol{q}_r=[x_e,y_e,\theta_e]^T \tag{3}$$

When the WCR is working on large oil tanks to detect defects, the area of the work space is large enough compared to the robot. Therefore, the work area is approximately regarded as a 2D plane region. Obviously, in this way, we can think of the working environment as a plane, the reference system (x, y) is used to define the local coordinate system used in this study, where x and y respectively represent the horizontal and vertical directions [6].

The sensors of WCR are used to measure the velocity and angle in the working environment and record the relevant information. The measured results of these data are used as a priori condition of the STEKF algorithm to calculate the information at the next moment. Then the kinematic discrete time equation of the robot in the two-dimensional plane is as follows,

$$\begin{aligned}x_k&=x_{k-1}+t\cdot\hat{v}_k\cdot cos\hat{\theta}_k+t\cdot\hat{\omega}_k\cdot sin\hat{\theta}_k\\ y_k&=y_{k-1}+t\cdot\hat{v}_k\cdot sin\hat{\theta}_k-t\cdot\hat{\omega}_k\cdot cos\hat{\theta}_k\\ \theta_k&=\hat{\theta}_k\end{aligned} \tag{4}$$

where $\boldsymbol{x}_k=[x_k,y_k,\theta_k]^T$ respectively represent the position in the horizontal direction, the position in the vertical direction, and the motion angle; k represents the step size, and the parameter t is the

ISSN: 2414-1895 DOI: 10.6919/ICJE.202105_7(5).0012

sampling period during the operation. The $\hat{v}_k$ and $\hat{\omega}_k$ respectively represent the linear velocity and angular velocity [7].

The partial derivative matrix of the nonlinear process function is as follows,

$$\boldsymbol{F}_{x_k} = \begin{bmatrix} 1 & 0 & -t \cdot \hat{v}_k \cdot \sin\hat{\theta}_k + t \cdot \hat{\omega}_k \cdot \cos\hat{\theta}_k \\ 0 & 1 & t \cdot \hat{v}_k \cdot \cos\hat{\theta}_k + t \cdot \hat{\omega}_k \cdot \sin\hat{\theta}_k \\ 0 & 0 & 1 \end{bmatrix}; \boldsymbol{F}_{w_k} = \begin{bmatrix} t \cdot \cos\hat{\theta}_k & t \cdot \sin\hat{\theta}_k & 0 \\ t \cdot \sin\hat{\theta}_k & -t \cdot \cos\hat{\theta}_k & 0 \\ 0 & 0 & 1 \end{bmatrix} \quad (5)$$

Where the symbol $\hat{}$ denotes the measurement data from the WCR sensors.

2.2 Introduction of two filtering algorithms

2.2.1. EKF

The filtering theory originally proposed by Kalman is only applicable to linear systems. To break through this limitation, Kalman filtering theory was further applied to the nonlinear field, thus giving birth to the EKF filter theory. The EKF filtering theory can be formulated as follows,

Time update:

$$\hat{\boldsymbol{x}}_{k|k-1} = f(\hat{\boldsymbol{x}}_{k-1|k-1}, \boldsymbol{u}_k) \quad (6)$$

$$\boldsymbol{P}_{k|k-1} = \boldsymbol{F}_k \boldsymbol{P}_{k-1|k-1} \boldsymbol{F}_k^T + \boldsymbol{Q}_k \quad (7)$$

$$\hat{\boldsymbol{y}}_k = \boldsymbol{z}_k - \boldsymbol{H}_k \hat{\boldsymbol{x}}_{k|k-1} \quad (8)$$

$$\boldsymbol{S}_k = \boldsymbol{H}_k \boldsymbol{P}_{k|_{k-1}} \boldsymbol{H}_k^T + \boldsymbol{R}_k \quad (9)$$

Measurement update:

$$\boldsymbol{K}_k = \boldsymbol{P}_{k|_{k-1}} \boldsymbol{H}_k^T \boldsymbol{R}_k^{-1} \quad (10)$$

$$\hat{\boldsymbol{x}}_{k|k} = \hat{\boldsymbol{x}}_{k|_{k-1}} + \boldsymbol{K}_k \hat{\boldsymbol{y}}_k \quad (11)$$

$$\boldsymbol{P}_{k|k} = (\boldsymbol{I} - \boldsymbol{K}_k \boldsymbol{H}_k) \boldsymbol{P}_{k|_{k-1}} \quad (12)$$

Where $\hat{\boldsymbol{x}}_{k|k-1}$ and $\boldsymbol{P}_{k|k-1}$ are respectively the predicted state vector and corresponding predicted error covariance matrix, $\boldsymbol{u}_k$ is the controller vector, $\boldsymbol{F}_k$ is the transformation matrix, $\boldsymbol{Q}_k$ is the process noise covariance matrix, $\boldsymbol{R}_k$ is the measurement noise covariance matrix, $\hat{\boldsymbol{x}}_{k|k}$、$\boldsymbol{P}_{k|k}$ are respectively the state estimate vector and corresponding estimation error covariance matrix, $\boldsymbol{K}_k$ is the Kalman gain, and $\boldsymbol{H}_k$ denotes the Jacobian matrix of the range measurement function. In addition, $(\cdot)-1$ denotes the inversion operation of a matrix.

2.2.2. Student's t distribution

Extended Kalman Filter with the Student's t distribution (STEKF) is an algorithm proposed based on EKF by assuming that both the process and measurement noises are Student's t distributions, which can further improve the calculation accuracy of the state estimation and the noise error covariance matrix.

We give the definition of the Student's t distribution: $\mathbf{x} = [x_1, \ldots x_{n_{dx}}]^T$ as an n_{dx}-D random vector, $\hat{\mathbf{x}}$ is the mean vector and $\mathbf{P}$ is the symmetric matrix, the multivariate Student's t distribution to describe the process noise $\boldsymbol{w}_k$ and the measurement noise $\boldsymbol{v}_k$ as follows [9],

$$\boldsymbol{St}(\boldsymbol{x}, \hat{\boldsymbol{x}}, \boldsymbol{P}, \upsilon) = \frac{\Gamma\left(\frac{\upsilon+n}{2}\mathrm{dx}\right)}{\Gamma\left(\frac{\upsilon}{2}\right)} \frac{\left(1+\frac{(\boldsymbol{x}-\hat{\boldsymbol{x}})^T \boldsymbol{P}^{-1} (\boldsymbol{x}-\hat{\boldsymbol{x}})}{\upsilon}\right)^{-\frac{\upsilon+n}{2}\mathrm{dx}}}{(\pi\upsilon)^{\frac{n}{2}\mathrm{dx}} \sqrt{|\boldsymbol{P}|}} \quad (13)$$

where $\Gamma(r) = \int_0^\infty e^{-t}\, t^{r-1}\mathrm{dr}$ is the Gamma function, υ is used to determine the tail behavior of the density. One thing that needs special attention the covariance matrix $\boldsymbol{P}$ is not the covariance matrix of the random vector $\boldsymbol{x}$, and when $\upsilon > 2$ the covariance matrix of the random vector $\boldsymbol{x}$ is related as follows [10],

ISSN: 2414-1895 DOI: 10.6919/ICJE.202105_7(5).0012

$$E[(\mathbf{x}-\hat{\mathbf{x}})(\mathbf{x}-\hat{\mathbf{x}})^T] = \frac{\upsilon}{\upsilon-2}\mathbf{P} \tag{14}$$

2.2.3. A Fuzzy Adaptive Extended Kalman Filter with the Student's t distribution

A new statistical model based Student's t distribution can better maintain the robustness and accuracy of the algorithm. To be specific, an adaptive fuzzy control approach is designed to improve the robustness and accuracy of the algorithm in the time update and measurement update in the STEKF algorithm. To address the influence of noise on the STEKF, we deal with the measurement noise covariance matrix $\boldsymbol{R}_k$ by exploiting an adaptive fuzzy method.

Table 1. The Fuzzy rule table

Input-2(ec) \ Input-1(e)	NL	NM	NS	Z	PS	PM	PL
NL	7	7	6	6	5	5	4
NM	7	6	6	5	5	4	3
NS	6	6	5	5	4	3	3
Z	6	5	5	4	3	3	2
PS	5	5	4	3	3	2	2
PM	5	4	3	3	2	2	1
PL	4	3	3	2	2	1	1

The fuzzy rule table is shown in Table 1. The NB, NM, NS, PB, PM, PS and Z respectively represent negative big, negative middle, negative small, positive big, positive middle, positive small and zero. The Input-1 and Input-2 represent two different input values, respectively [5]. $\boldsymbol{P}_{k|\text{k-1}}$, $\boldsymbol{P}_{\text{k-1}|\text{k-1}}$ and $\boldsymbol{z}_k$, $\boldsymbol{z}_{k|\text{k-1}}$ are selected as fuzzy controller influence factors, respectively, and the adaptive factor ξ_1 are obtained by using a doubleinput-single-output fuzzy controller. The optimized new Rf can be obtained by multiplying ξ_1 with the $\boldsymbol{R}_k$.

Meanwhile, we consider to retain the heavy-tailed posterior density throughout time, so we should prevent the growth of the dof, thus we builds up the scalar factor m to adjust the initial update result [7]. Here, the moment matching method is adopted to find the scalar factor m. We have $\boldsymbol{P}_{\text{k-1}|\text{k-1}}\frac{\eta_{k-1}}{\eta_{k-1}-2} = m\boldsymbol{P}_{\text{k-1}|\text{k-1}}\frac{\hat{\eta}_{k-1}}{\hat{\eta}_{k-1}-2}$, and when $\eta_{k-2} > 2$, where $\hat{\eta}_{k-1} = min(\hat{\eta}_{k-1}, \upsilon)$.

Time update:

$$\hat{\boldsymbol{x}}_{k|k-1} = f(\hat{\boldsymbol{x}}_{k-1|k-1}, \boldsymbol{u}_k) \tag{16}$$

$$\boldsymbol{P}_{k|k-1} = \boldsymbol{F}_k\boldsymbol{P}_{k-1|k-1}\boldsymbol{F}_k^T + \boldsymbol{Q}_k \tag{17}$$

$$\hat{\boldsymbol{y}}_k = \boldsymbol{z}_k - \boldsymbol{H}_k\hat{\boldsymbol{x}}_{k|k-1} \tag{18}$$

$$\boldsymbol{R}_f = \xi_1 \cdot \boldsymbol{R}_k \tag{19}$$

$$\hat{\boldsymbol{S}}_k = \boldsymbol{H}_k\boldsymbol{P}_{k|_{\text{k-1}}}\boldsymbol{H}_k^T + \boldsymbol{R}_k \tag{20}$$

Measurement update:

$$\boldsymbol{K}_k = \boldsymbol{P}_{k|_{\text{k-1}}}\boldsymbol{H}_k^T\boldsymbol{R}_k^{-1} \tag{21}$$

$$\hat{\boldsymbol{x}}_{k|k} = \hat{\boldsymbol{x}}_{k|_{\text{k-1}}} + \boldsymbol{K}_k\hat{\boldsymbol{y}}_k \tag{22}$$

$$\boldsymbol{\Delta} = (\boldsymbol{z}_k - \boldsymbol{z}_k^-)^T\boldsymbol{S}_k^{-1}(\boldsymbol{z}_k - \boldsymbol{z}_k^-) \tag{23}$$

$$\hat{\boldsymbol{P}}_{k|k} = (\boldsymbol{I} - \boldsymbol{K}_k\boldsymbol{H}_k)\boldsymbol{P}_{k|_{\text{k-1}}}\frac{\eta_{k-1}+\boldsymbol{\Delta}}{\eta_{k-1}+\eta_{\text{dz}}} \tag{24}$$

$$\boldsymbol{P}_{k|k} = m\hat{\boldsymbol{P}}_{k|k} + (1-m)(\boldsymbol{P}_{k|_{\text{k-1}}} - \boldsymbol{K}_k\boldsymbol{S}_k\boldsymbol{K}_k^T) \tag{25}$$

ISSN: 2414-1895 DOI: 10.6919/ICJE.202105_7(5).0012

where the linearized measurement matrix is the Jacobian matrix of the measurement equation as $\boldsymbol{H}_k = \frac{\partial h}{\partial x_k}$.

3. Simulations and results

We consider the problem of tracking an agile target in two-dimensional space executing a manoeuvring turn with unknown and time-varying turn rate, and the target is observed in clutter. The process and measurement models are given by[8],

$$\boldsymbol{x}_k = \begin{bmatrix} 1 & \frac{\sin \Omega T_0}{\Omega} & 0 & \frac{\cos \Omega T_0 - 1}{\Omega} & 0 \\ 0 & \cos \Omega T_0 & 0 & -\sin \Omega T_0 & 0 \\ 0 & \frac{1-\cos \Omega T_0}{\Omega} & 1 & \frac{\sin \Omega T_0}{\Omega} & 0 \\ 0 & \sin \Omega T_0 & 0 & \cos \Omega T_0 & 0 \\ 0 & 0 & 0 & 0 & 1 \end{bmatrix} \boldsymbol{x}_{k-1} + \boldsymbol{w}_{k-1} \tag{26}$$

$$\boldsymbol{z}_{\mathrm{i,k}} = \tan^{-1}\left(\frac{\eta_k - s_\eta^i}{\varsigma_k - s_\varsigma^i}\right) + \boldsymbol{v}_{\mathrm{i,k}} (i = 1,\ldots,5) \tag{27}$$

where the state vector $\boldsymbol{x}_k = [\varsigma \quad \dot{\varsigma} \quad \eta \quad \dot{\eta} \quad \Omega]^T$,$\boldsymbol{x}_k$, ς and η denote positions, and $\dot{\varsigma}$ and $\dot{\eta}$ denote velocities in the x and y directions, respectively, and Ω represents a constant but unknown turn rate, and $T_0 = 1\,s$ denotes the sampling interval of the measurements, and $\boldsymbol{z}_{\mathrm{i,k}}$ and $\boldsymbol{v}_{\mathrm{i,k}}$ are the measurement and measurement noise of sensor i, respectively.

The outlier corrupted process noise $\boldsymbol{w}_k$ and measurement noise $\boldsymbol{v}_k$ are uncorrelated white processes, they are generated according to the following rules [8],

$$\boldsymbol{w}_k = \begin{cases} N(\boldsymbol{0}, \boldsymbol{Q}) & \text{w.p.0.95} \\ N(\boldsymbol{0}, 50\boldsymbol{Q}) & \text{w.p.0.05} \end{cases}, \boldsymbol{v}_k = \begin{cases} N(\boldsymbol{0}, \boldsymbol{R}) & \text{w.p.0.95} \\ N(\boldsymbol{0}, 50\boldsymbol{R}) & \text{w.p.0.05} \end{cases} \tag{28}$$

where w. p. denotes "with probability". Equations (17) mean that wk and vk are most from a Gaussian distribution with nominal covariance matrix Q or R and 5 percent of process and measurement noise values are from Gaussian distributions with the severely increased covariance matrix. The noises of process and measurement, which are generated in terms of (17), have heavy tails. In this simulation, we chose $\upsilon = 6$ and parameters $T_0, \boldsymbol{Q}, \boldsymbol{R}, \boldsymbol{x}_0, \boldsymbol{P}_{0|0}$ ·as defined in [6].

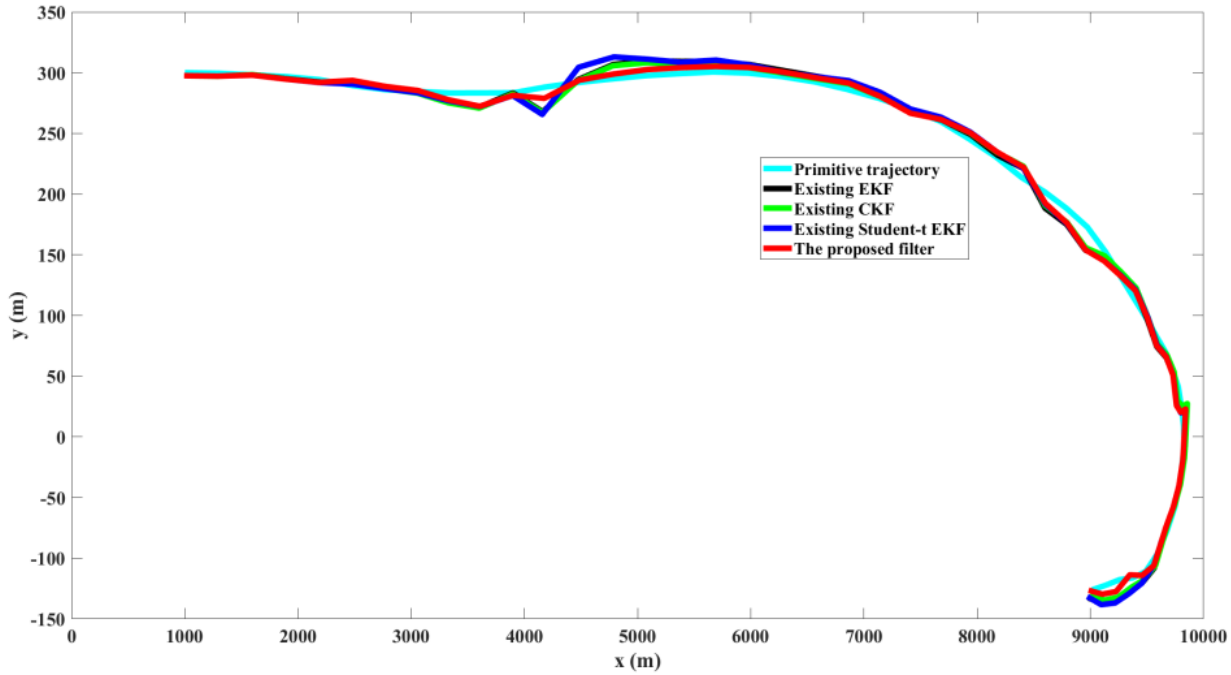

Figure 1. True and estimated trajectories of the target

ISSN: 2414-1895 DOI: 10.6919/ICJE.202105_7(5).0012

3.1 Trajectories of the target

In order to intuitively compare the calculation results of WCR motion trajectory under three different filtering algorithms, this section will list the real motion trajectory of the WCR, the motion trajectory of the CKF algorithm, EKF algorithm and STEKF algorithm. The results are as follows,

It is seen from Figure 1 that the estimated trajectories from the STEKF methods are closer to the true trajectory as compared with CKF and EKF methods. However, there are still some cases in which the simulation result of the STEKF deviated greatly in some time periods. In terms of stability, the EKF algorithm is recommended to ensure the stable operation of the filtering method.

3.2 Implementation times of the single step run

The true and estimated trajectories obtained from the proposed filter and the CKF, EKF and STEKF in a single Monte Carlo run are shown in Table 2. The results are as follow,

Table 2. Implementation Times of the Algorithms in a Single Step Run

Filters	CKF	EKF	STEKF	The proposed filter
Time (s)	1.137×10^{-2}	2.951×10^{-3}	2.980×10^{-3}	1.652

Table 2 is the comparison of implementation times of the algorithms in a single step run, the optimization of the proposed algorithm makes the tracking effect significantly improved, but the implementation times of the algorithms in a single step run is also longer. The longer the operation time, the more difficult the calculation is, but the positioning accuracy is impacted. However, under different experimental conditions, the longer the operation time means the lower the operation efficiency.

3.3 Root mean square error

To compare the performances of the proposed filters with existing filters, the root-mean-square errors (RMSEs) of the position, velocity and turn rate are chosen as performance metrics. To compare the performances of the proposed filters with existing filters, the RMSEs of the position, velocity and turn rate are chosen as the performance metrics. The RMSE of position is defined as follows [7],

$$RMSE_{\text{pos}}(k) = \sqrt{\frac{1}{M}\sum_{S=1}^{M}((\varsigma_k^S - \hat{\varsigma}_k^S)^2 + (\eta_k^S - \hat{\eta}_k^S)^2)} \tag{29}$$

where M = 1000 denotes the number of Monte Carlo runs, and T=50s denotes the simulation time, $(\varsigma_k^S, \eta_k^S)$ and $(\hat{\varsigma}_k^S, \hat{\eta}_k^S)$ respectively, denote the true and estimated positions at the S-th Monte Carlo run. Similar to the RMSEs in position, we can also formulate the RMSEs in velocity and turn rate.

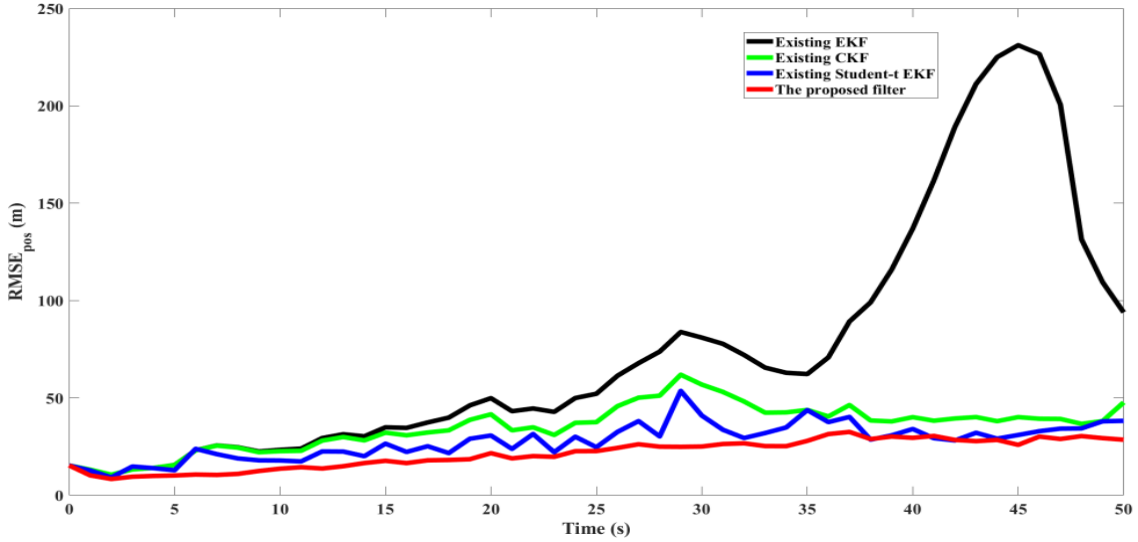

Figure 2. RMSEs of the position of the target

ISSN: 2414-1895 DOI: 10.6919/ICJE.202105_7(5).0012

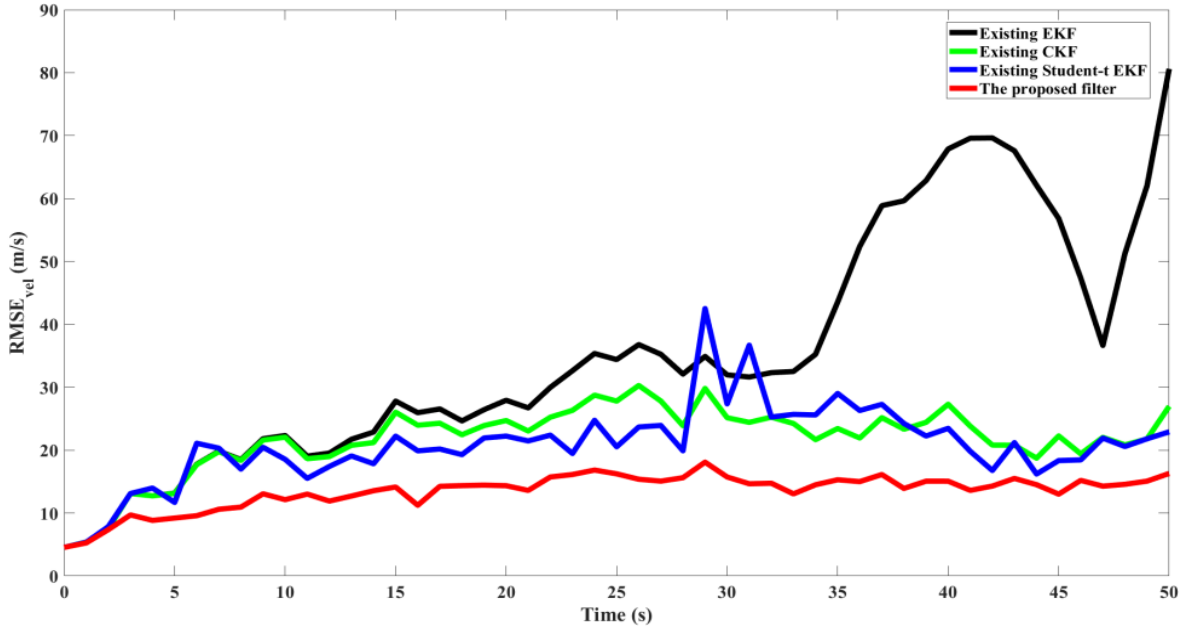

Figure 3. RMSEs of the velocity of the target

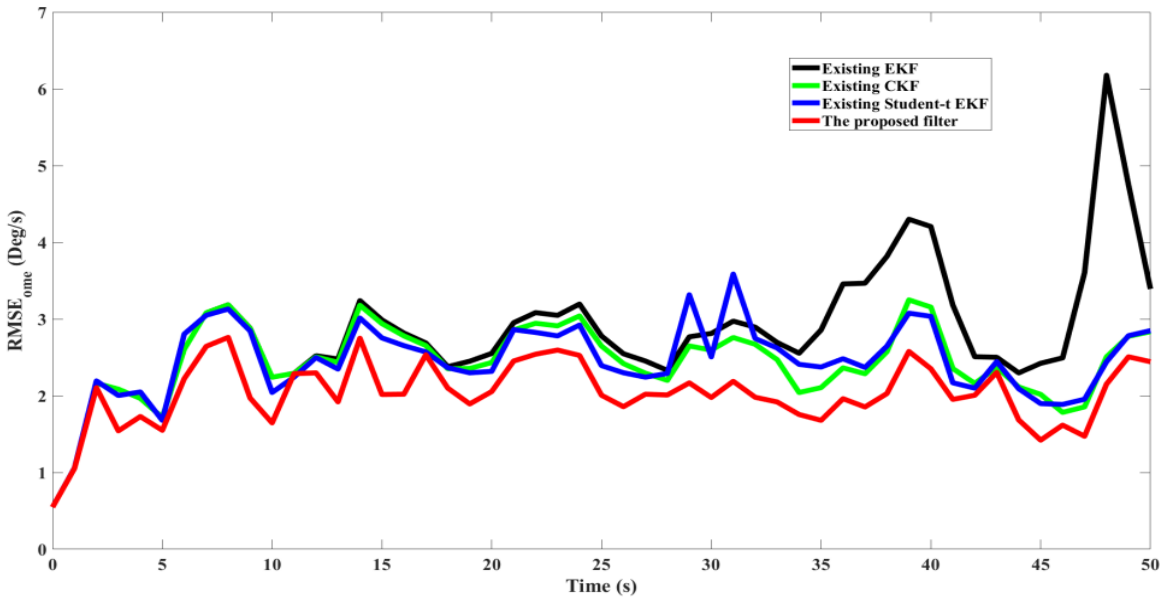

Figure 4. RMSEs of the turn rate of the target

The RMSEs and of position, velocity and turn rate from the proposed filters and existing filters are, respectively, shown in Figure 2, 3 and 4.

We can see from Fig. 2–Fig. 4 that the proposed filter has considerably improved filtering accuracy as compared to the existing CKF, EKF and the STEKF.

The RMSEs of the position and velocity from the proposed filter ang the existing CKF, EKF, STEKF increase abruptly after 15s since they are specially designed for Gaussian process and measurement noises so that they are sensitive to process and measurement outliers. The RMSEs of the turn rate from the proposed filter also increase abruptly in 0~5s, which is incurred by the truncation errors of the first-order linearisation. Moreover, the RMSEs from the CKF, EKF and STEKF are different since they assume a well-behaved process and measurement noise, but we see that they are sensitive to process and measurement outliers from experiments.

ISSN: 2414-1895 DOI: 10.6919/ICJE.202105_7(5).0012

4. Conclusion

In this paper, the proposed an adaptive robust Student's t-based extended Kalman filter. The measurement noise of the inspection WCR trajectory tracking is expressed by introducing a Student's t distribution. The simulation results show that the proposed algorithm is obviously better than the CKF, EKF and STEKF. Our proposed lateral comparison method can be reflected effectively in the operational effect of the filtering algorithm by the simulations. This paper proposed method can be applied to optimization and comparison of other types of filters in the WCR trajectory tracking research field.

References

[1] B. D. O. Anderson, J. B. Moore, and M. Eslami. "Optimal filtering", IEEE Transactions on Systems, Man, and Cybernetics, vol. 12, no. 2, pp. 235–236, Mar. 1982.

[2] S. Julier, J. Uhlmann, and H. F. Durrant-Whyte. "A newmethod for the nonlinear transformation of means and covariances in filters and estimators", IEEE Transactions onAutomatic Control, vol. 45, no. 3, pp. 477–482, Mar. 2000.

[3] I. Arasaratnam and S. Haykin. "Cubature Kalman filters", IEEE Transactions on Automatic Control, vol. 54, no. 6, pp. 1254–1269, June 2009.

[4] Y. L. Huang and Y. G. Zhang. "A new process uncertainty robust Student's t based Kalman filter for SINS/GPS integration", IEEE Access, vol. 5, no. 7, pp. 14391–14404, Jul. 2017.

[5] Q. Li, Y. Ben, S. M. Naqvi, J. A. Neasham, and J. A. Chambers. "Robust student'st-based cooperative navigationfor autonomous underwater vehicles", IEEE Transactions onInstrumentation and Measurement, vol. 67, no. 8, pp. 1762–1777, Aug. 2018.

[6] K. Kobayashi, Ka Cheok, and K. Watanabe. "Estimationof absolute vehicle speed using fuzzy logic rule-based kalmanfilter", in Proceedings of 1995 American Control Conference -ACC'95, vol. 5, pp. 3086 – 3090, Seattle, WA, USA, June 1995.

[7] Q. Li. and Y. Ben and J. Tan and N. S. Mohsen and C. Jonathon. "Robust Selection of the Degrees of Freedom in the Student'st Distribution Through Multiple Model Adaptive Estimation", Signal Processing, vol. 153, no. 7, pp. 255 - 265, Oct. 2018.

[8] M. Roth, E. Özkan, F. Gustafsson, "A Student's t filter for heavy-tailed process and measurement noise", 2013 IEEE International Conference on Acoustics, Speech and Signal Processing (ICASSP) (IEEE, Vancouver, BC, 2013), pp. 5770–5774.

[9] S. Kotz and S. Nadarajah, "Multivariate T-Distributions and Their Applications". Cambridge, U.K.: Cambridge Univ. Press, 2004.

[10] Y. Huang, Y. Zhang, N. Li, S. M. Naqvi, and J. Chambers, "A robust Student's t based cubature filter," in Proc. Int. Conf. Inf. Fusion (FUSION), Jul. 2016, pp. 9–16.